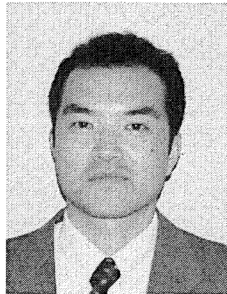


A STUDY ON THE STRUCTURAL EVALUATION OF A THIN CEMENT CONCRETE OVERLAY

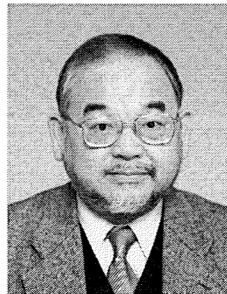
(Translation from Proceedings of JSCE, No.641/V-46, 39-52, 2000.2)



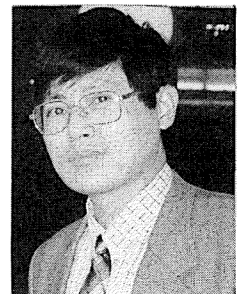
Hiromitsu NAKANISHI



Shinich TAKEI



Teruhiko MARUYAMA



Boming TANG

One method of rehabilitating an existing asphalt pavement is to place a thin cement concrete overlay on top of the asphalt concrete pavement. This rehabilitation method has been the subject of various research and development work over the past twenty years in Japan. However, this failed to make the method popular. One reason for this is that it was not established as a design procedure for pavements. In this research, the theory of a beam on a Winkler foundation is first applied and a stress analysis procedure of pavement slabs is examined. Next, taking the degree of bonding between these two layers into consideration, a model of the composite structure consisting of a thin cement concrete layer and the existing asphalt pavement layer is examined. The results of these two examinations are combined, and a design procedure for thin layer cement concrete overlays as a composite pavement is established.

Keywords: white-topping, thin layer concrete overlay, bonding coefficient, bending stress, shear stress, winkler foundation

Hiromitsu Nakanishi is a division manager at the Engineering Research Laboratory of Taiyu Kensetsu Co., Ltd., Nagoya, Japan. He obtained his Dr. Eng. from Nagaoka University of Technology in 2000. His research interests relate to cement concrete pavements and asphalt concrete pavements. He is a member of the JSCE.

Shinich Takei is a researcher at the Engineering Research Laboratory of Taiyu Kensetsu Co., Ltd., Nagoya, Japan. His research interests relate to cement concrete pavements and asphalt concrete pavements.

Teruhiko Maruyama is a Professor in the Department of Civil and Environmental Engineering at Nagaoka University of Technology (Nagaoka, Niigata, 940-2188 Japan).

He specializes in pavement engineering, traffic control, and the road environment. He graduated from the Tokyo Institute of Technology in 1969 and obtained his doctorate degree in 1981 based on research on the fatigue properties of asphalt mixtures.

Boming Tang is a Vice-Director of the China Chong Qing Highway Bureau (Chong Qing 400067, China). He specializes in the planning, design, construction, and maintenance of highways. He graduated from South East University in Nanjing, China in 1985 and obtained his doctorate degree in 1990 based on research on the structural estimation of concrete pavements. He also worked as an associate professor at Nagaoka University in Japan from 1995.

1. INTRODUCTION

A thin cement concrete overlay, called White-topping in the West, is one of the available rehabilitation methods for an asphalt pavement. The concrete is thinly overlaid onto an existing asphalt pavement. The thin layer of cement concrete is from 5cm to 15cm thick in general, and is constructed on the assumption that it adheres perfectly to the conventional asphalt surface. In the West, the method has been in use since about 1960, and its long-term serviceability has been proved [1], [2], [3].

Usage of this construction method is increasing. Although in Japan it was researched and some test pavements were laid in about 1980, since then construction has come to a half. It is supposed that this has happened because the expected durability of the pavement on site was not always achieved. However, steel fiber reinforced concrete (SFRC) used as a thin overlay ($t=10\text{cm}$) [4] when constructing National Highway Route-23 in March 1981, where the authors were also engaged in construction, stood up under heavy traffic for 15 years until renewed in 1996.

In recent years, because extended pavement life is desired, this rehabilitation method has suddenly come into focus, and research [5], [6] has recently started again. The most important reason for the thin-layer cement concrete overlay method not becoming popular was its failure to satisfy long-term durability requirements. This was because no technique for rational structure evaluation leading to appropriate designs for particular situations had been established.

The establishment of such a design method for this rehabilitation technique requires solutions to many issues; a design method for wheel load stress, a design method for temperature stress, problems related to the shrinkage of cement concrete materials, problems with joints, and others. The scope of this paper is limited to the wheel load stress, and research is carried out as follows. First, a calculation method for bending stress in the thin-layer cement concrete pavement is proposed. Second, this method is extended for application to the composite slab. Third, a calculation method for shear stress between the upper layer and the lower layer of the two-layer structure is proposed. The results of this research are reported in this paper.

2. PREVIOUS RESEARCH AND PURPOSE OF THIS RESEARCH

2.1 Previous Research

In Japan, the present design equation for cement concrete pavements was proposed by Dr. S. Iwama. It was derived by modifying Westergaard's equation and Teller & Sutherland's equation so that the loading state can be adjusted. Verification was carried out using cement concrete slab from 19.9cm to 24.9cm in thickness. As regards composite slabs, Dr. T. Fukuda presented an evaluation method [8]. According to this theory, the neutral axis of the composite slab is calculated, and an equivalent thickness double the depth to the neutral axis is assumed. Here, although the neutral axis is calculated from a balance of fiber stresses in the direction of a principal axis, the balance between the moment imposed by external forces and the moment caused by fiber stresses on the neutral axis is not considered. Therefore, even if bending stresses for an equivalent thickness are calculated, because the flexural rigidity differs, problems with calculation accuracy remain.

In the Outline for Airport Concrete Pavement Structure Design, Fukuda's theory progressed further in that adhesive imperfection at interface had been taken into consideration and also the geometrical moment of inertia had been considered in the composite beam. However, a calculation method for the bending moment generated in the pavement is not specifically given. In fact, it is difficult to calculate the bending moment in a pavement slab, and also it is difficult to use this theory in actual pavement design. In the case of a lean cement concrete with a specified elastic modulus for the lower layer, Packard [10] has presented a table of properties for an equivalent section when the interface adhesion ratio is 50% or 100% from both of theory and experiment. However, the results are not arranged in the form of a general equation with consideration of the degree of adhesion at the interface, so their practical use is limited.

Since it is necessary to take the influence of interface adhesion into consideration in order to establish a future design method for thin-layer cement concrete overlays, research related to the shear stress acting on the interface is also essential. An equation for calculating the shear stress generated in a composite structure has been proposed in the Japan Patent Official Report [11]. In this document, the shear stress generated by wheel loading

at the interface in the composite structure is expressed as a difference in fiber stresses at the lower face of the upper layer and at the top surface of the lower layer. Although this viewpoint is adopted in the latest Japanese investigations [5], [12], and also in research [13] by T. J. Larsen in U.S, the method is questionable.

On the other hand, R.K. Ghosh, et al. [14], [15] have also given a calculation method for shear stress induced by wheel loading, proposing a method for determining the stress caused by shrinkage of the layer above the interface in the composite structure. However, it is inapplicable to the situation studied in this research at the point where elastic modulus differs and the bonding of the interface cannot be considered. Moreover, what is calculated here is the shear stress that is generated directly under the boundary of the loading area in the width direction, when wheel loading acts on the free edge of the pavement slab.

Moreover, since the main purpose of the conventional design method for cement concrete pavements is to calculate the bending stress under wheel loading, we have to depend on numerical analysis techniques such as FEM to find the stress distribution induced by the wheel load. In research by T. Nishizawa, et al. [16] elastic plane FEM was used to develop analysis methods for composite pavements, in cases of both full bonding and full non-bonding of the two layers. Later they studied how to handle the interface bonding state using FEM. In terms of midstates between full bonding and full non-bonding, research is under way.

On the other hand, regarding the analysis of cement concrete pavements, R. Hudson, et al. [17] assumed a concrete pavement to be an assembly of elements consisting of rigid bars, elastic joints, and twisting bars. According to their analysis method, although the composite slab and bonding at the interface is not taken into consideration and its structure is very complicated, dividing the pavement slab into a limited number of bar elements is useful. As this makes clear, there is insufficient consideration of the degree of bonding at the interface of a composite slab in existing research, and a practical design method for a thin cement concrete overlay has yet to be established yet.

2.2 Purpose of This Research

The main purpose of this research is to calculate the stress and strain induced in a thin cement concrete overlay by wheel loading, and also the shear stress generated at the interface with the asphalt pavement. Furthermore, in order to develop the study to include load transmission at joints, etc. in the future, it is necessary to understand the distribution of bending stress or shear stress.

The long-term durability of this rehabilitation method depends on how the thin cement concrete layer (Co) and the lower asphalt concrete layer (As) behave together. The unity of the two layers relates closely with the rigidity of the composite structure itself, and affects the bending stress and shear stress induced on the undersurface of the cement concrete layer or at the interface. However, the conventional design method fails to consider this point, and is premised on full bonding. Hence, if full bonding is not achieved in an actual pavement, the actually generated stress will be greater than the designed stress. That is, there is a risk the design erring on the side of danger. To take into account the degree of unity, it is necessary to calculate the bending moment or shear stress generated in the pavement.

To do this, the authors refer to the research by R. Hudson, et al. and simplify it further, carrying out the investigation as follows:

- (1) Considering the pavement slab to be an assembly of beams on a Winkler foundation, the application of beam theory to the slab is examined.
- (2) Taking a composite beam in which the degree of bonding at the interface is considered, calculation methods for the bending and shear stress are examined.
- (3) The results of (1) and (2) are combined, and its potential as a design method for wheel loading stress in the thin-layer cement concrete overlay is examined.

3. WHEEL LOAD STRESS IN THIN CEMENT CONCRETE SLAB

3.1 Combined Beam Structure (Combined Beam Method)

The cement concrete pavement is to be analyzed as a slab on a Winkler foundation. However, the analysis of a slab taking into consideration the degree of bonding at the interface is very difficult. For this reason, the

pavement slab is divided into two or more elements as shown in Fig-1 and the theory of a beam on a Winkler foundation is applied to each beam element. The combined beam structure is assumed to consist of a main beam and two or more side beams placed on a Winkler foundation. By setting up boundary conditions for the main beam and the side beams, the rigidity of the combined beam structure is approximated to that of the slab.

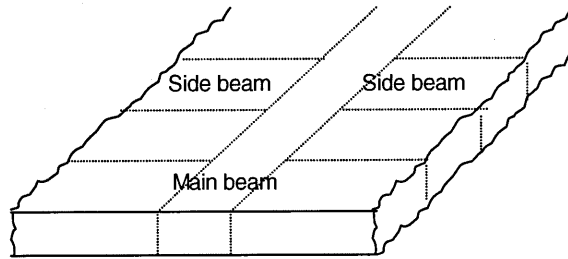


Fig-1 Concept of combined beam structure

3.2 Modeling Combined Beam structure

Fig-2 shows the linkage state between the main beam and the side beams. As the main beam, an infinite beam, a half-infinite beam, or a finite beam might be considered. The side beams, also, could be half-infinite beams or finite beams. Moreover, the side beams could be arranged either on one side of the main beam or on both sides of the main beam. And the combination of the main beam and the side beams can be chosen pertinently by a loading state to calculate, i.e. a central loading, a free edge loading, a corner loading, etc. A shear force and a bending moment are basically transmitted to the side beams from the main beam through the links. In this model, load transmission between side beams is not taken into consideration. However, the rigidity of the actual slab and that of the combined beam structure can be equaled by deciding on a suitable width of the side beams using Eq-(8), as mentioned later.

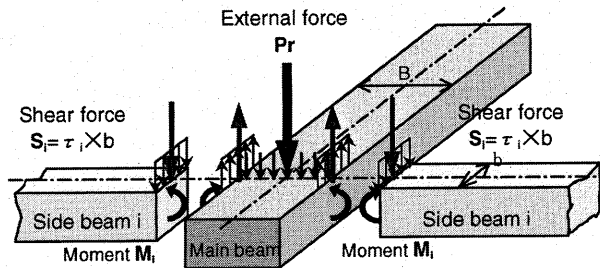


Fig-2 Modeling of combined beam structure

It is assumed that the wheel load on the pavement slab acts only on the main beam, and also the stress calculation is performed for the main beam. That is, if all wheel loads are regarded as external forces, and the shear force and moment transmitted from side beams as external forces, the bending moment and shear force as well as the deflection induced in the main beam can be calculated. First, the shear force (S_i) at a link to a side beam is calculated. Regarding the shear stress per unit length (τ_i) as an unknown, the deflection of the main beam at the link is calculated by regarding this shear force as an external force. In terms of the side beam, considering that the shear force is the same magnitude as that in the main beam and in the opposite direction, and that it acts on the edge of the side beam, the deflection at the link with the main beam is calculated. With regard to the moment generated at the link, it should for strictness be derived such that the slope of the main beam in the direction of the side beam is equal to the slope of the side beam. However, it is not easy to derive the slope in the direction intersecting perpendicularly with the principal axis of the main beam. Moreover, when considering the moment, if the side beams act on one side of the main beam (when assuming a free edge), a torque will act on the main beam, and calculation will become difficult. Consequently, the moment is treated as follows to manage these problems.

When the side beams are on both sides of the main beam (Refer to Fig-2), the slope at the wheel loading center in the direction of the side beam is naturally zero because of the symmetrical structure. Therefore, if the width of the main beam is reduced, the slope at the link with the side beam can be assumed to be zero. That is, the

moment which causes the slope at the end of the side beam to be zero is assumed. However, even if this moment acts on the main beam, it is assumed that the bending moment and the shear force in the direction of the principal axis of the main beam is not influenced. Moreover, when the main beam has side beams on one side only (assuming a free edge or a corner), the moments in the links between the main beam and the side beams can be considered to be nearly zero if the width of the main beam is considered to be narrow. Therefore, these moments are ignored in this case.

3.3 Application to Free Edge

A conceptual outline of application of the combined beam structure to a free edge is shown in Fig-3 and Fig-4. If the main beam and the side beams are pulled apart in section e-e of Fig-3, the situation appears as shown at the top of Fig-4. The lower diagram in Fig-4 shows section f-f of Fig-3. The shear force (S_i) and moment (M_i) ought to act naturally at the joint face between the main beam and a side beam. However, the moment at the joint can be ignored to obtain an approximation if the main beam width is made narrow. Therefore, only the shear force needs to be taken into consideration. Moreover, the wheel load as the external force is considered a group of the line loads acting only on the main beam. Moreover, taking the double tire of a heavy vehicle as the wheel load, the area of contact can be considered a rectangle with reference to survey data, as shown in Fig-5. The line load (P_r) and the load spacing (m_p) are defined as in Eq-(1) and Eq-(2).

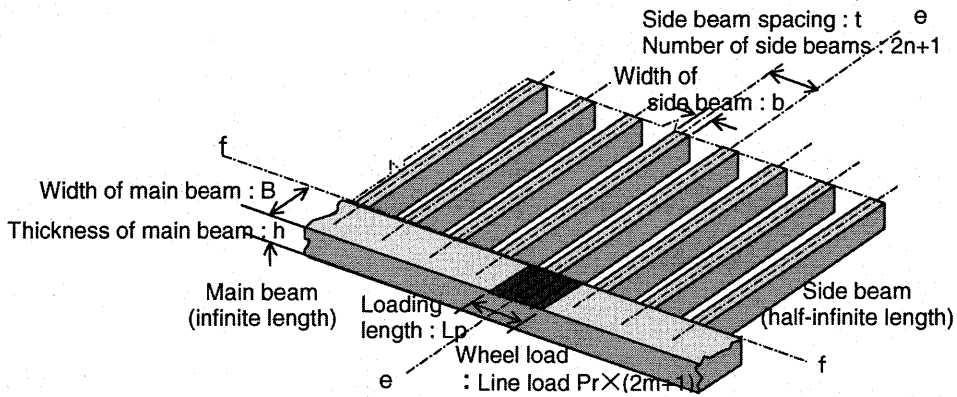


Fig-3 Example of application to free edge of combined beam structure

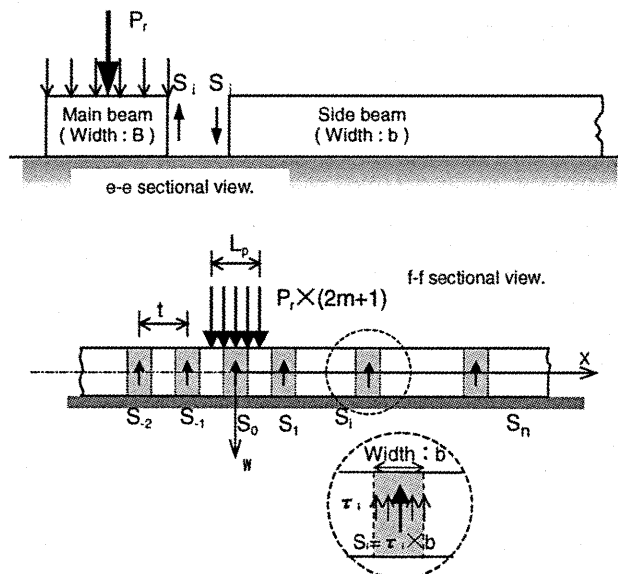


Fig-4 External force acting on main beam

$$P_r = \frac{p \times (L_p \times B)}{2m+1} \text{----- (1)}$$

$$m_p = \frac{L_p}{2m} \text{----- (2)}$$

where,

- P_r : Line load (N)
- m_p : Line load spacing (mm)
- p : Contact pressure (N/mm²)
- L_p : Contact length (mm)
- B : Width of main beam (mm)
- $2m+1$: Number of line loads (considering symmetry)
- r : Subscript for line load ($r = -m, \dots, 0, \dots, m$)

Assuming that the external force (P_r) and the shear force ($S_i \ i = 0, 1, 2, \dots, n$) act on the main beam as shown in Fig-4, the deflection of the main beam at the center of the joint face with each side beam can be expressed as a function of the shear stresses ($\tau_i \ i = 0, 1, 2, \dots, n$) acting at the center of the joint face. The deflection of the main beam at a joint with a side beam is then as given by Eq-(4), as derived from the basic equation [18] of a beam of infinite length on a Winkler foundation.

$$\phi = \sqrt[4]{\frac{k}{4EI}} \text{----- (3)}$$

$$w_{it} = \frac{pL_p\phi}{2(2m+1)K_{75}} \sum_{r=-m}^m F_1\{abs(rm_p - it)\} - \frac{b\phi}{2BK_{75}} \sum_{j=-n}^n \tau_j F_1\{abs((-i+j)t)\} \text{----- (4)}$$

where,

- w_{it} : Deflection of position i (mm)
- $F_1(x) = e^{-\phi x} (\cos \phi x + \sin \phi x) \quad x \geq 0$
- $abs(x)$: Absolute value of x
- K_{75} : Coefficient of base support value for base course (N/mm³)
- p : Contact pressure due to wheel load (N/mm²)
- E : Elastic modulus of beam material (N/mm²)
- k : Multiple of K_{75} and beam width (N/mm²)
- I : Geometrical moment of inertia of beam (mm⁴)
- $2n+1$: Number of side beams
- t : Side beam spacing (mm)

The other symbols are as for Fig.-4 and Fig.-5.

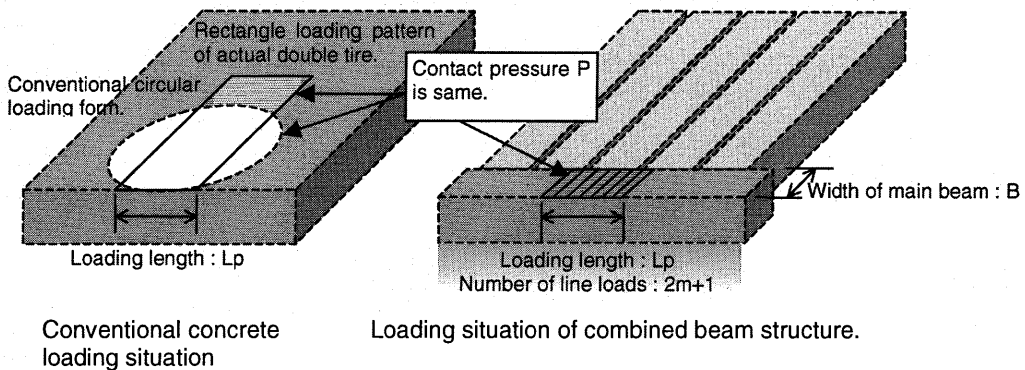


Fig-5 Wheel loading

Since the main beam is symmetrical, the following equation can be given; $\tau_j = \tau_{-j}$, $F_1(x) = F_1(-x)$. Therefore, Eq-(4) results in (n+1) equations for (n+1) unknowns (τ_j $j=0, 1, \dots, n$). The 1st term of Eq-(4) represents the deflection due to the wheel load external force, and the 2nd term is the deflection resulting from shear stresses at the joints with side beams. On the other hand, the deflection of the side beam at joint j ($=i$), where the main beam joins a side beam, can also be expressed as a function of the shear stress (τ_j). On the side beam, the shear stress as an external force is considered as acting on the end of the side beam. In connection with the side beam (j), the deflection at the end (W_j $j=0,1,\dots,n$) can be expressed as in Eq-(5) from the basic equation [18] of a beam of half-infinite length on a Winkler foundation.

$$w_j = \frac{\tau_j \phi}{2K_{75}} [AF_1(0) - 2BF_2(0) + F_1(0)] \text{-----} (5)$$

where,

$$F_1(x) = e^{-\phi x} (\cos \phi x + \sin \phi x) \quad F_2(x) = e^{-\phi x} \sin \phi x \quad F_3(x) = e^{-\phi x} (\cos \phi x - \sin \phi x) \quad F_4(x) = e^{-\phi x} \cos \phi x$$

$$A = F_3(0) + 2F_4(0) \quad B = F_3(0) + F_4(0)$$

x : Distance in principal direction (in this case, $x=0$)

The other symbols are the same as given previously.

If n+1 simultaneous equations are solved under conditions where the deflection (W_{it}) of the main beam at point (i) by Eq-(4) is equal to the deflection (W_j) of the side beam (j) by Eq-(5), the unknown shear stresses (τ_j $j=0,1,2,\dots,n$) can be calculated. Further, if the shear stress calculated above is considered to be the external forces acting on the main beam, the bending moment and shear force generated in the main beam can be calculated.

$$M(x) = \frac{pL_p B}{4(2m+1)\phi} \sum_{r=-m}^m F_3\{abs(x-rm_p)\} - \frac{b}{4\phi} \sum_{j=-n}^n \tau_j F_3\{abs(x-jt)\} \text{-----} (6)$$

$$S(x) = -\frac{pL_p B}{2(2m+1)} \sum_{r=-m}^m sign(x-rm_p) F_4\{abs(x-rm_p)\} + \frac{b}{2} \sum_{j=-n}^n sign(x-jt) \tau_j F_4\{abs(x-jt)\} \text{-----} (7)$$

where,

x : Position along principal axis (where the external force loading position is the origin)

$M(x)$: Bending moment (N·mm) at position x

$S(x)$: Shear force (N) at position x

$abs(\xi)$: Absolute value of (ξ)

$sign(\xi)$: 1 for $\xi \geq 0$, -1 for $\xi < 0$

The other symbols are as given previously.

The first term on the right-hand side of Eq-(6) and Eq-(7) represents the deflection due to wheel load external force, and the 2nd term is that due to the shear stress generated in the joint with a side beam, respectively.

3.4 Examination of Calculation Result by Combined Beam Method

As indicated by Eq-(4), the factors affecting calculation accuracy are the ratio (b/B) of side beam width to main beam width, the number (n) of side beams, and the side beam spacing (t), in the case of a combined beam structure for a free edge. When (b/B) approaches zero, the bending moment at the center of the wheel load becomes equal to that of a beam without side beams. Conversely, when (b/B) approaches infinity, the bending moment calculated at the center of the wheel load converges on zero. That is, in this Combined Beam Method, (b/B) can be considered a constant related to the rigidity of the structure. Therefore, through comparison with other calculation results and actual measurements, the most suitable value of (b/B) will be determined.

Fig-6 shows the relationship between (b/B) and ϕ . In this figure, the wheel load is 49kN, the contact pressure (p) is 0.54N/mm², the main beam width (B) is 100mm, the number of side beam (n) is 100, and side beam spacing (t) is 50mm. Then, (b/B) was reverse-calculated so that the wheel load stress calculated using the Combined Beam Method equals that calculated using the equation given in the Manual for Cement Concrete Pavement on various combinations, i.e. slab thickness, elastic modulus, and the base support value of the base course. The equation of this relation is shown in Eq-(8).

$$\frac{b}{B} = 2.7 \times 10^{-5} \times \left(\frac{1}{\phi}\right)^{1.42} \text{-----(8)}$$

Fig-7 and Fig-8 show the relationships between the number of side beams and the bending moment calculated by the Combined Beam Method, in the case of the main beam width (B) of 100mm and the side beam spacing (t) of 50mm. Fig-9 and Fig-10 show the relationships between number of side beams and the shear force calculated by the Combined Beam Method, in the case of the main beam width (B) of 100mm and the side beam spacing (t) of 50mm. As above, if the main beam has 50 or more side beams attached, the calculated value converges toward a fixed value.

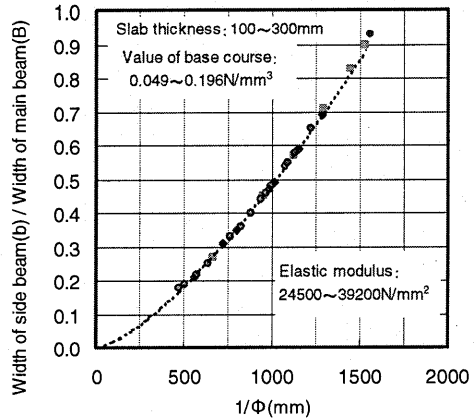


Fig-6 Relation between ϕ and b/B

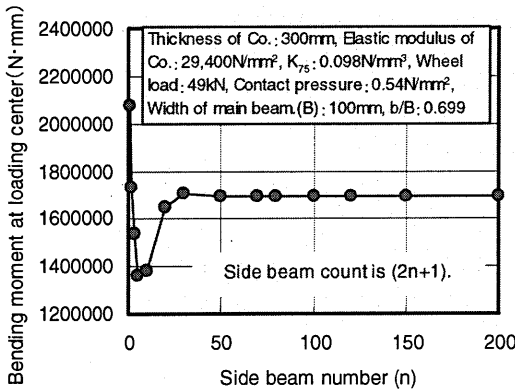


Fig-7 Bending moment at loading center and number of side beams

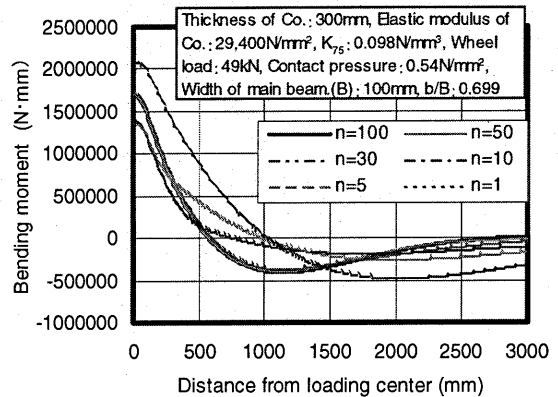


Fig-8 Bending moment diagram and side beam count

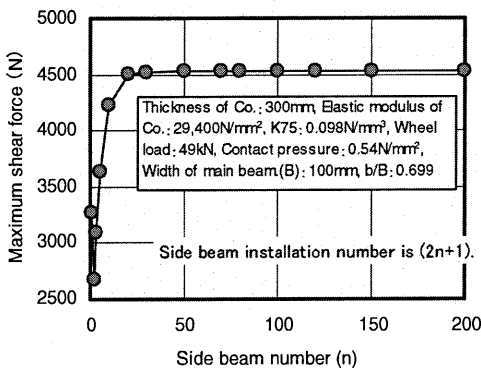


Fig-9 Maximum shear force and side beam count

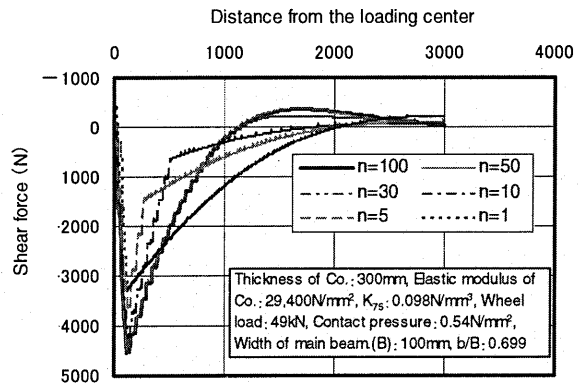


Fig-10 Shear force diagram and side beam count

This result shows that main beam width of 100mm, a side beam spacing of 50mm, and 100 side beams are suitable calculation conditions for the Combined Beam Method. Although the load in the Combined Beam Method has already been given, in order to check the influence of concrete slab thickness on the calculation result, a comparative calculation is carried out under the conditions shown in Table -1. The results are shown in Fig-11. As this shows, the calculation result by the Combined Beam Method is in close agreement to the calculation result, assuming that a suitable value of (b/B) given by Eq-(8) is used. However, for thin layer slabs with a thickness of under 50mm, the behavior given by the Combined Beam Method differs from that obtained with the conventional equation in the Manual for Cement Concrete Pavement. In the case of this manual, the bending stress at the underside of the slab becomes compressive beyond a certain thickness. In contrast, with the Combined Beam Method, the bending stress at the underside is increasingly tensile.

Although the method of calculation in the Combined Beam Method differs completely from the conventional approach in the Manual for Cement Concrete Pavement, the calculation conditions and parameters are determined such that the calculated wheel load stress directly under the loading point is equivalent. Therefore, application in the range where the results by the two methods differ, such as for a thickness of 50mm or less, there is a need to collect and analyze survey data from now on. At the present time, the application range for the Combined Beam Method should be considered to be from 50mm to 300mm in equivalent thickness of the cement concrete slab. The influence of wheel load on the calculated wheel load stresses directly under the load by the Combined Beam Method is checked in Fig-12.

The results calculated by the Combined Beam Method are mostly in agreement with the Manual for Cement Concrete Pavement. The above discussion demonstrates that the slab problem can be converted into a beam problem by using the Combined Beam Method. Furthermore, it turns out that the calculated wheel load stress is almost equivalent to that obtained by the conventional equation in the Manual for Cement Concrete Pavement. Consequently, the bending moment generated at the pavement free edge, the shear force, and their distributions are also easily calculable.

Table-1 Conditions for free edge stress calculation of concrete

	Equation of pavement guideline	Combined Beam Structure
Base support value. (N/mm ³)	0.049, 0.098, 0.196	0.049, 0.098, 0.196
Thickness of Co.(mm)	20~300	20~300
Elastic modulus of Co.(N/mm ²)	29,400	29,400
Poisson's ratio of Co	0.25	-
Wheel load.(kN)	49	49
Shape of contact area	Circle (Radius of 17cm)	Rectangle* (20.2×45cm)
Side beam count n	-	100
Side beam spacing : t (mm)	-	50

* Actually measured double tire grounding area (5t load) at 5°C

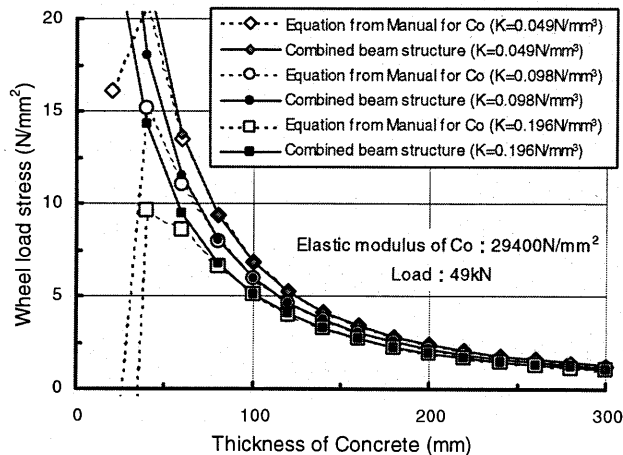


Fig-11 Relation between thickness of concrete and wheel load stress calculated by conventional method and Combined Beam Method

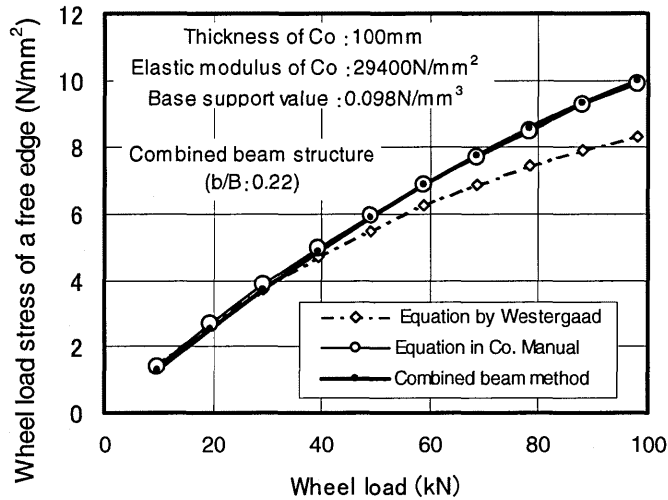


Fig-12 Relation between wheel load and wheel load stress calculated by conventional method and Combined Beam Method

4. COMPOSITE BEAM WITH CONSIDERATION OF BONDING AT INTERFACE

4.1 Basic Equation

Where a thin-layer cement concrete pavement is constructed on an asphalt pavement, there is no guarantee of being able to maintain the ideal of a composite slab; that is, full adhesion of the thin cement concrete to the lower asphalt concrete layer. The actual state of the bond depends on conditions such as temperature, loading speed, treatment of the asphalt surface, problems during construction, and so on. Generally, a state between full bonding and full non-bonding should be examined.

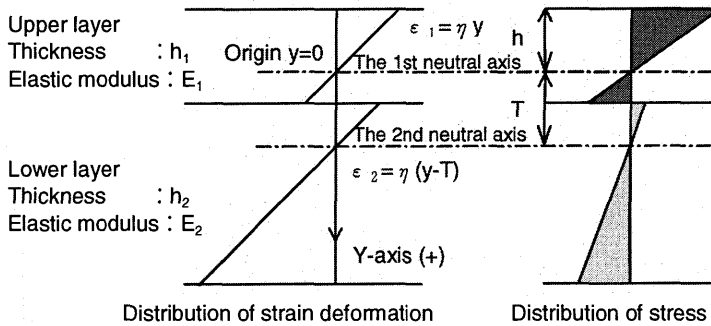


Fig-13 Complexity of imperfect adhesion condition

In the full bonding state, only one neutral axis can be determined at a particular position. In the full non-bonding state, two neutral axes develop and the axes are considered to form at the mid-position of each layer. In all cases, the distribution of strain is assumed to depend on the Bernoulli-Euler's Assumption. Moreover, if it is assumed that the two layers deform with the same curvature, the distributions of the two strains in the composite slab must have the same slope.

Fig.-13 shows an imperfect bonding state between full bonding and full non-bonding. As this shows, when the position of the 1st neutral axis is assumed to be the origin of the coordinate axes, the 2nd neutral axis develops at distance (T) from the origin. The strain distribution (ϵ_1) in the upper layer and that in the lower layer (ϵ_2) can be expressed respectively as follows:

$$\varepsilon_1 = \eta y \text{-----} (9)$$

$$\varepsilon_2 = \eta(y - T) \text{-----} (10)$$

$$T = (1 - t_b) \left(\frac{h_1 + h_2}{2} \right) \text{-----} (11)$$

Where,

t_b : Bonding coefficient at the interface. ($t_b = 0 \sim 1$, $t_b = 0$ for full non-bonding, $t_b = 1$ for full bonding)

T : Distance between neutral axes.

The other symbols are as shown in Fig.-13.

If the equilibrium equation in the axial direction is solved and arranged, the position (h) of the 1st neutral axis from the upper surface is given by Eq-(12).

$$h = \frac{h_1 + \alpha \beta h_2 + 2\alpha h_2 - 2\alpha \beta T}{2(1 + \alpha \beta)} \text{-----} (12)$$

Where,

$$\alpha = E_2 / E_1, \quad \beta = h_2 / h_1$$

h : Distance from upper surface to first neutral axis.

Moreover, the external force moment and the moment of internal fiber stress about the neutral axis must be in balance. If calculation is carried out with the sum of the moment of the upper layer to the first axis and that of lower layer to the second axis in balance with the external force moment, the result can be arranged as follows:

$$J = \frac{b}{3} \left\{ (h_B^3 - h_A^3) + \alpha (h_C^3 - h_B^3) - 3T\alpha (h_C^2 - h_B^2) + 3T^2\alpha (h_C - h_B) \right\} \text{-----} (13)$$

Where, $h_A = -h$, $h_B = -h + h_1$, $h_C = -h + h_1 + h_2$

B : Width of beam (cm), T : distance between neutral axes.

$$\text{and,} \quad \eta = \frac{M}{E_1 J} \text{-----} (14)$$

That is, it is conceivable that (J) calculated here is the geometrical moment of inertia for the composite beam with consideration of bonding. Therefore, in calculating a composite beam on a Winkler foundation in consideration of bonding, the value of (J) acquired using Eq (13) should be used as the geometrical moment of inertia.

4.2 Stress and Strain of composite beam with consideration of bonding

The strain and stress in any section of the composite beam can be calculated with bonding taken into consideration using Eq-(9), Eq-(10), and Eq-(11) from the above paragraph.

$$\varepsilon_1 = \frac{M}{E_1 J} \cdot y \text{-----} (15)$$

$$\sigma_1 = \frac{M}{J} \cdot y \text{-----} (16)$$

provided that $-h \leq y \leq -h + h_1$

$$\varepsilon_2 = \frac{M}{E_1 J} \cdot (y - T) \text{-----} (17)$$

$$\sigma_2 = \frac{M\alpha}{J} \cdot (y - T) \text{-----} (18)$$

provided that $-h + h_1 \leq y \leq -h + h_1 + h_2$

4.3 Shear Stress at Interface of Composite Beam with Consideration of Bonding

The shear stress (τ) can be calculated from an equilibrium equation [19] for fiber stress (σ_x , $\sigma_x - d\sigma_x$) in a tiny element (dx) in direction x of the beam. The equilibrium equation for the element shown in Fig.-14 can be rearranged to give a general equation of shear stress (Eq-(19)). If Eq-(19) is applied to a composite beam with consideration of bonding, the shear stress of the upper layer is obtained as follows:

$$\therefore \tau = \frac{1}{b} \int_{(A)} \frac{d\sigma_x}{dx} dA \quad \text{----- (19)}$$

Applying Eq-(19) to a composite beam in consideration of bonding, the shear stress in the upper layer is as follows:

$$\tau = \frac{S}{2J} (y^2 - h^2) \quad \text{----- (20)}$$

provided that $(-h \leq y \leq -h + h_1)$

Similarly, that in the lower layer is as follows:

$$\tau = \frac{S}{2J} ((-h + h_1)^2 - h^2) + \frac{\alpha S}{2J} \{(y - T)^2 - (-h - T + h_1)^2\} \quad \text{----- (21)}$$

provided that $(-h + h_1 \leq y \leq -h + h_1 + h_2)$

The distribution of shear stress in the direction of thickness in the composite beam can be obtained from Eq-(20) and Eq-(21). The shear stress at the interface in the case of a thin-layer cement concrete overlay can be expressed by Eq-(22).

$$\tau_{in} = \frac{S}{2J} ((-h + h_1)^2 - h^2) \quad \text{----- (22)}$$

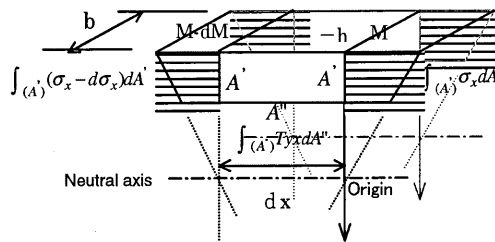


Fig-14 Shear stress

4.4 Composite Beam Structure in Consideration of Bonding

If details of the section of the thin-layer cement concrete overlay and the bonding coefficient at the interface are known, the geometrical moment of inertia can be calculated from Eq-(11), Eq-(12), and Eq-(13). If this value of (J) is used instead of the geometrical moment of inertia (I) in Eq-(3) and the Combined Beam Method is applied, the bending moment (M(x)) and shear force (S(x)) generated at the free edge can be calculated from Eq-(6) and Eq-(7). The wheel load stress can be found by substituting the bending moment into Eq-(16) and Eq-(18). Moreover, the shear stress induced by the wheel load can be found by substituting the shear force into Eq-(20), Eq-(21), and Eq-(22).

Although the most popular equation used to calculate wheel load stress on composite pavements depends on Fukuda's theory, the moment equilibrium condition is not taken into account by this method. However, supposing a virtual section in which the geometrical moment of inertia is equivalent with that obtained from Eq-(13), if the equation of Manual for Cement Concrete Pavement is applied to this virtual section and the result obtained is converted to a composite slab, the wheel load stress induced at undersurface of a composite pavement taking the geometrical moment of inertia into consideration can be calculated. Fig-15 shows the relationship between wheel load stress calculated using this method and that calculated by the Combined Beam Method. The results differ considerably from those obtained by the conventional method in which the geometrical moment of inertia is not taken into consideration. However, it turns out that the results obtained by the Combined Beam Method are the almost same as those by the conventional equation when the geometrical moment of inertia is taken into account.

Regarding the calculation of shear stress inside the pavement, the equation by Ghosh et al. [14], [15] for a single slab is the only one available method. However, Ghosh's equation calculates the shear stress in the direction of road width, while the Combined Beam Method calculates it on a free edge in the length direction. Fig-16 shows the calculated shear stress of a single slab with various properties using both methods. Although the calculated values naturally differ, the relationship between the two methods is almost directly proportional, as shown in Fig-16.

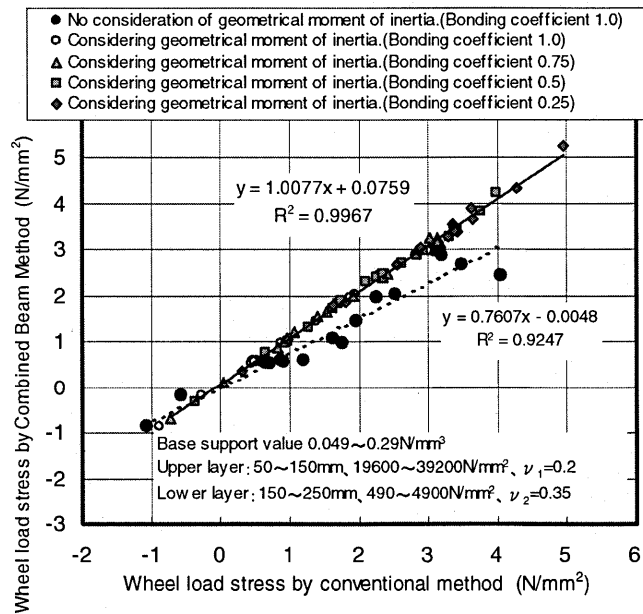


Fig-15 Comparison of calculation results by conventional method and Combined Beam Method (Wheel load stress)

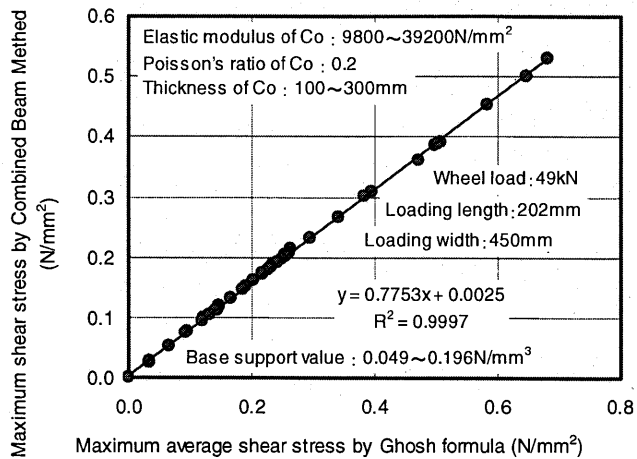


Fig-16 Comparison of calculated results by conventional method and combined beam structure (Shear stress)

5. VERIFICATION OF THIN-LAYER OVERLAY BY TEST CONSTRUCTION

5.1 Test Constructions

In order to verify the applicability of the technique that has been described here, test construction of thin-layer cement concrete overlays was carried out, and the strains were measured. The types of test construction are listed in Table-2. A high-vibration-compacted SFRC and an ordinary SFRC are used as the cement concretes, and two overlay thicknesses of 100mm and 150mm are adopted.

Moreover, three different interface treatment methods between the cement concrete layer and the asphalt concrete layer are tested. First, the conventional asphalt concrete surface is removed (A in Table-2). The surface is then grooved to a depth of 30mm at 1m spacing in the transverse direction using a diamond cutter. A steel plate 50mm in width is inserted into the groove as a binding plate (B1 in Table-2). Similarly a steel plate 65mm in width is inserted (B2 in Table-2). Similarly a steel plate 75mm in width is inserted (B3 in Table-2). Furthermore, a waterproofing paper layer is placed over the surface not being removed in order to disturb the bonding on purpose (C in Table-2).

Table-2 Test constructions

Thickness of Co.(mm)	100			150				
Thickness of As.(mm)	150							
Elastic modulus of Co.(N/mm ²)	43,900		34,800		34,800			
Interface processing	A	A	A	B1	B2	B3	B2	C
Base support value. (N/mm ³)	0.25		0.20	0.44		0.41		0.39
Test section No.	I	II	III	IV	V	VI	VII	VIII
Construction width (m)	3.6		3.6			3.6		
Construction extension (m)	32	9	9	9	9	5	5	10

5.2 Strain Measurements and Bonding Coefficient

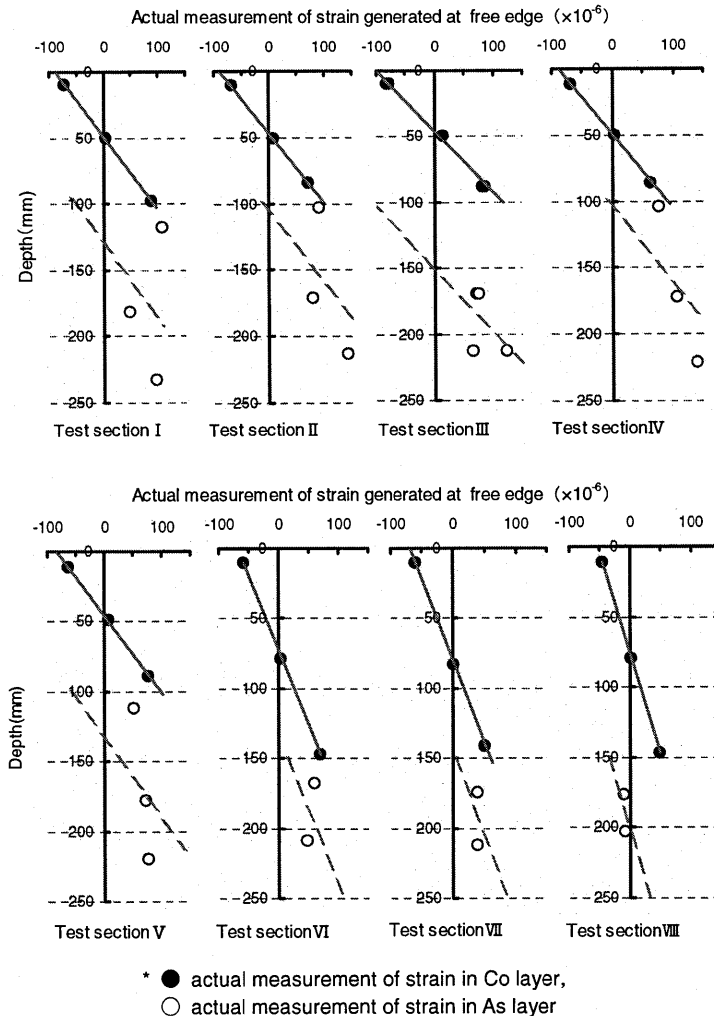


Fig-17 Actual measurements of strain and regression lines

Strain measurements were performed using a buried gauge (BS-8FT) laid into the cement concrete, and a line gauge (PL-60-11-3LT; Tokyo Sokki Research Institute) affixed to the pavement end section just before strain measurements. The lower asphalt concrete layer was cut such that the cut position matched the end of the upper cement concrete. Strain gauges were affixed at three positions on the cement concrete layer and asphalt concrete layer: upper, center, and lower on the side faces. As the loading vehicle used for measurements, the rear wheels of an 8t dump truck (single axle) were adjusted to 49kN. The contact area was 45cm in width by 20.2cm in length, and the contact pressure was 0.54N/mm². The loading position was immediately above the strain gauge, and the loading time was about 10 seconds. The strain measurements for static loading only are shown in Fig-17.

The solid line and dashed line shown in the figure are regression lines calculated from the actual strain measurements. Since the Bernoulli-Euler's Assumption, that is to remain plane and normal to the reformed neutral axis, holds almost in the strain distribution in the cement concrete layer, the measurements are approximated to a straight line and the position of first neutral axis can be found. The strain distribution in the lower asphalt concrete layer does not necessarily hold to the Bernoulli-Euler's Assumption. Moreover, the strain distribution of the asphalt concrete layer is not parallel to that of the cement concrete layer. It is thought that this is why the tensile strain expanding the cutting plane outside and the creep deformation generated in the asphalt concrete layer by the static loading.

However, as long as Fig.-17 is checked, the composite slab theory based on the conventional assumptions, i.e., the Bernoulli-Euler's Assumption and the full bonding state, does not hold. Therefore consideration in calculations to deal with this problem is needed. The concept of a bonding coefficient as examined in this paper is one proposal for dealing with this problem. The equation proposed here is based on the Bernoulli-Euler's Assumption on the premise that the upper layer and lower layer have strain distributions with the same curvature. Therefore, the calculation method is based on the assumption that the strain distribution in the asphalt concrete layer and that in the cement concrete layer have the same slope, and the position of the second neutral axis is calculated on this basis. The bonding coefficient (tb) is then calculated using Eq-(11) from the separation (T) between the two neutral axes. The results are shown in Table-3.

The bonding coefficient at the interface between the cement concrete layer and the asphalt concrete layer in the case of removing the asphalt concrete surface, which is the conventional interface treatment method, can be estimated at no more than 0.34 on average. On the other hand, the bonding coefficient when bonding plates are used at the interface is 0.46, so is a little higher on average. When a waterproofing paper is used, the results indicated that no composite slab-action can be expected.

Table-3 Treatment interface and bonding coefficient

test section	Co./As. processing method of interface	position of neutral axis		separation between two acquired neutral axis (T)	Bonding coefficient	
		first neutral axis	the second neutral axis		(tb)	Ave
I	A	48.6	130.6	82.0	0.34	0.34
II	A	46.8	106.8	60.0	0.52	
III	A	46.1	152.9	106.8	0.15	
IV	B1	49.2	105.4	56.2	0.55	0.46
V	B2	45.6	134.4	88.8	0.29	
VI	B3	72.9	134.4	61.5	0.51	
VII	B2	80.3	14.61	65.8	0.47	
VIII	C	76.2	201.2	125.0	0	

5.3 Evaluation of Elastic Modulus of Asphalt Concrete Layer

Next, the elastic modulus of the asphalt concrete layer was examined using the bonding coefficient derived above. Results obtained in a follow-up survey [21] on an SFRC thin-layer overlay (t = 100mm) pavement constructed on National Highway Route 23, as mentioned in the introduction, was used as the data for this examination. The follow-up survey entailed measuring the relationship between strains on the undersurface of the cement concrete layer under 5t static wheel loading and temperature of the asphalt concrete layer. The Combined Beam Method is applied to this pavement with an interface bonding coefficient of 0.34, as obtained in this examination, and the

elastic modulus of the asphalt concrete layer is reverse-calculated such that the measured strain and the calculated strain are equal. The results are shown in Fig.-18.

The authors estimate that the elastic modulus of this asphalt concrete layer was about 0-700N/mm² without consideration of the bonding coefficient in a previous report [22]. However, it turns out that it can be estimated at 200-2700N/mm² after taking the bonding coefficient into consideration in this examination. The relationship between temperature of the asphalt concrete layer and the elastic modulus of the asphalt concrete layer is obtained as Eq-(23), below.

$$E_{as} = -59.194T_{as} + 2691 \text{ ----- (23)}$$

Where,

E_{as} : Elastic modulus of asphalt concrete (N/mm²)

T_{as} : Temperature of surface of asphalt concrete layer (°C)

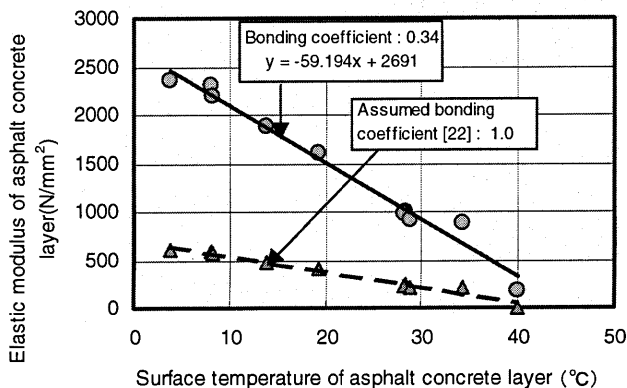


Fig-18 Surface temperature and elastic modulus of asphalt concrete layer

There have been many investigations resulting to the evaluation of the elastic modulus of asphalt concrete layers. Ueshita et al. [23] carried out a Benkelman-beam Deflection Test at a surface temperature of 22-24 °C, yielding an elastic modulus estimated at 784-1470N/mm² (converted to SI units by the authors). Although the loading conditions differ a little, this result and the results of our research are quite similar for similar temperature conditions.

Using a Dynaflect Test Machine, Sato et al. [24] determined the relationship between asphalt concrete temperature and elastic modulus, and they conclude that it is similar to the elastic modulus in Van der Poel's work. However, Sato's examination is carried out using a dynamic load with a number of vibrations at 8Hz, and the elastic modulus of the asphalt concrete layer is 4900N/mm² at 20 °C, so the modulus is quite large in comparison with the results under static loading in this research.

5.4 Adjustment between Survey Strain and Calculated Strain

Since the temperature on the upper surface of the asphalt concrete layer at the time of strain measurements was 19.5 - 20.5 °C, the temperature is considered to be 20 °C and the elastic modulus of the asphalt concrete layer is considered to be 1520N/mm² from Eq-(23). Moreover, a calculation is carried out using the values shown in Table-3 for the bonding coefficient and the values shown in Table2 for the other conditions related to the pavement. The conditions illustrated in Table -1 as calculation conditions for the Combined Beam Method are used, and the value of (b/B) obtained from Eq-(8) is applied.

Fig-19 shows the relationship between strain gauge values taken from the pavement edge and values calculated by the Combined Beam Method with consideration of bonding at the interface (○ mark in Fig.-1). Also in this figure, the relationship between the strain at the undersurface of the cement concrete, as calculated from a regression of strain measurements, and the calculated strain is shown (● mark in Fig-19). Furthermore, the relationship with strain calculated by the conventional method [20] on the assumption that the interface is fully bonded is shown (△,▲ mark in Fig.-19). For the tensile strain induced at the lower part and the undersurface

of the cement concrete, it turns out that the value measured actually fits better with the value calculated using the Combined Beam Method with consideration of the bonding at the interface than the value calculated using the conventional method presupposing full bonding. Moreover, the value of the tensile strain calculated by the conventional method is 10-20% smaller than the actually measured value. This must be the result of not taking the bonding coefficient into consideration.

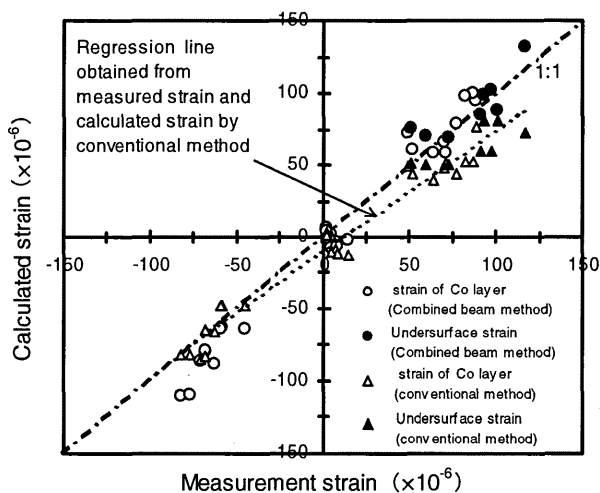


Fig-19 Relationship between actually measured strain and calculated values of strain

Next, the influence of loading position on the strain is measured. The wheel load is applied at position, 0cm, 40cm, 80cm, and 120cm from the position of the gauge in test section III and IV. The results are examined. Directly under the loading position, a differential arose between the distribution of strain in the cement concrete layer and the distribution of strain in the asphalt concrete layer, and the differential was transformed into the bonding coefficient. Consequently, although it was determined that the bonding coefficient in test section III was 0.15 and that in test section IV was 0.55, it turned out that the degree of bonding changed in company with movement of the loading position away from the gauge position.

Fig-20 shows the influence line diagrams for strain at the concrete layer undersurface. In the case where the loading position is 40, 80, or 120cm away from the strain gauge, agreement with the calculated value is mostly good in cases where the bonding coefficient is 1.0. From these results, it can be said that the bonding coefficient at the interface varies not only with interface treatment but also with loading conditions. That is, it is considered that the shear stress falls with distance from the loading position and the degree of bonding at the interface is approaching to the full bonding with decreasing of the shear stress.

Next, it is calculated how the strain generated at the cement concrete layer undersurface would change with bonding coefficient for each test section. Fig-21 shows the relationship between bonding coefficient and strain at the cement concrete undersurface. Moreover, the relationship between the bonding coefficient obtained from the actual measurements and the strain at the cement concrete undersurface, as inferred from the actual strain measurements, is also shown in this figure. These results show that the strain generated at the concrete layer undersurface changes greatly according to the bonding coefficient at the interface.

Test section III is most greatly influenced of the degree of interface bonding, i.e., the bonding coefficient, followed by test sections I, II, IV, and V. The thickness of the cement concrete layer is 10cm in all these test sections. Although cement concrete with the same elastic modulus is used in test sections III, IV, and V, the base support value of the base course in test sections IV and V is twice or more that of test section III. Moreover, the base support value in test sections III, I, and II is the same, but the elastic modulus of the cement concrete in test sections I and II is about 25% larger than that in test section III. The strain generated in the case of full non-bonding (bonding coefficient = 0) is about double in the case of full bonding (bonding coefficient = 1.0) in these test sections. The test section that is difficult to be influenced by the bonding coefficient is test section V, VI, and VII, where the cement concrete layer thickness is 15cm. It is

thought that when the upper concrete layer is thin, the elastic modulus is small, and the base support value is small, so it is easy for the bonding coefficient at the interface to be influenced. Thus, if the bonding coefficient is not taken into consideration in design, the reliability of the results obtained can be considered remarkably low.

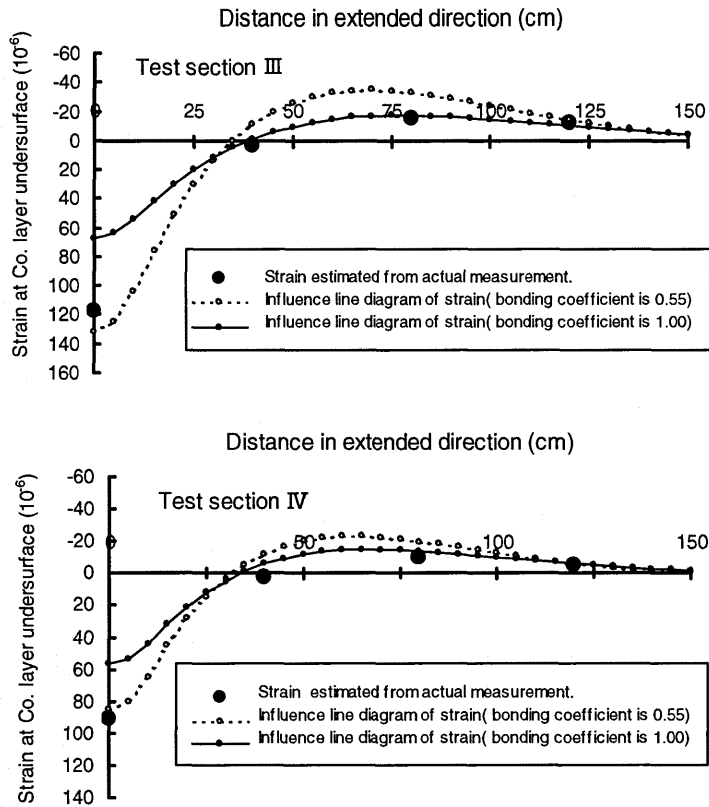


Fig-20 Influence line diagram of strain of concrete undersurface

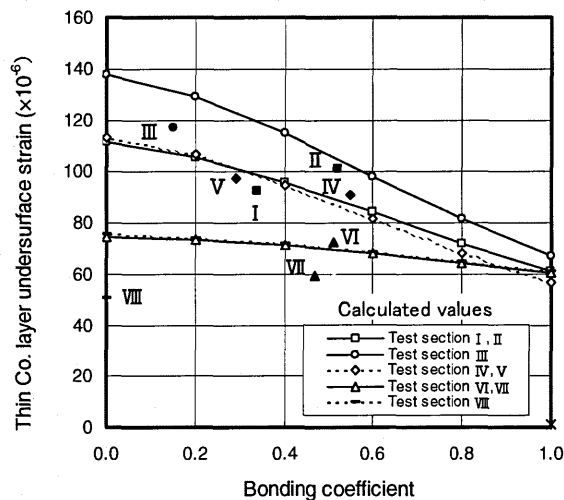


Fig-21 Bonding coefficient and strain of concrete undersurface

5.5 Shear Stress Generated in Pavement

Next, the results of examining the shear stress at the interface, which relates to the all-important bonding of the thin layer concrete overlay, are shown. First, the shear force ($S(x)$) generated in the main beam is calculated from Eq-(7) using the Combined Beam Method. Next, the shear stress is calculated from Eq-(20) and Eq-(21) using this shear forces. If the shear stress is calculated for test sections I - VIII, it becomes as in Fig-22. The distribution of shear stress describes the secondary parabola which shows the local maximum at the neutral axis as shown in Eq-(20) and Eq-(21). Since two neutral axes arise when full bonding is not achieved, although a local maximum is found at the position of the 2nd neutral axis, when this 2nd neutral axis is in the upper layer, no local maximum is found in the lower layer. When the bonding coefficient is 0 such as in test section VIII, the shear stress at the interface becomes 0 too.

Moreover, the relationship between bonding coefficient at the interface and shear stress at the interface is given by Eq-(22), and the results are shown in Fig. -23. The shear stress generated at the interface is, of course, small when the bonding coefficient is small, and the shear stress generated at the interface increases as the bonding coefficient increases. Moreover, since the shear stress reaches a peak at the neutral axis, when the position of the neutral axis approaches the position of the interface, a large shear stress arises at the interface. Although the value of this shear stress at the interface differs according to the structure and conditions of the test pavement, it is 0.15N/mm^2 at most at the interface when a 49kN wheel load acts.

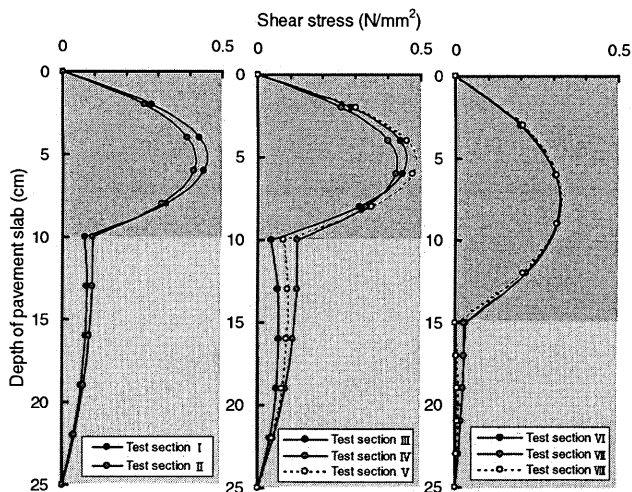


Fig-22 Shear stress for every test section

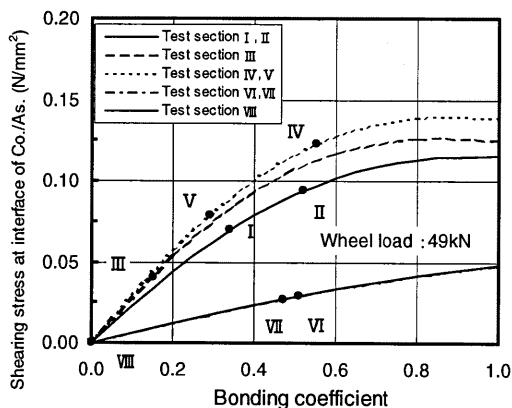


Fig-23 Bonding coefficient and shear stress for every test section

6. CONCLUSION

In order to evaluate the wheel load stress and the interface shear stress induced by wheel loading in a thin cement concrete overlay, an extension of composite beam theory to take into account bonding at the interface is examined. The conclusions are as follows:

- (1) It is possible to transpose a cement concrete pavement slab into a Combined Beam Structure on a Winkler foundation, and to carry out calculations on this basis. The method can be used for the design of thin-layer cement concrete overlays by incorporating consideration of bonding into the composite beam. Although the conventional design method can deal with only full bonding, design for arbitrary bonding conditions, as would arise in practice, is achieved using this method.
- (2) The bonding coefficient between the existing asphalt pavement surface and the thin-layer cement concrete overlay ranges from about 0.3 to about 0.5 directly under a static wheel load. However, the interface behaves almost as if full bonding is achieved at points 40cm or more distant from the load.
- (3) The elastic modulus of the asphalt concrete layer depends on temperature, measuring approximately 200-2700N/mm² when the temperature of the asphalt concrete surface is 0-40 °C. The strain and stress generated at the undersurface of the thin-layer cement concrete overlay vary greatly with the bonding coefficient at the interface. Therefore, the reliability of calculated values not taking the bonding coefficient into consideration may be very poor.
- (5) The shear stress generated at the interface between the existing asphalt concrete pavement and the thin-layer cement concrete overlay is about 0.15 N/mm² at most. However, when the elastic modulus of the asphalt concrete layer increases, i.e., under low temperatures, under dynamic loading, etc, the shear stress at the interface increases.

Acknowledgement

Dr. Norio Hasebe, professor at Nagoya Institute of Technology, provided much counseling and guidance in the development of the Combined Beam Method. We express our gratitude to him.

References

- [1] James D. Grove, Gary K.Harris and Bradley J. Skinner: Bond Contribution to Whitetopping Performance on Low Volume Roads, Construction Report for Iowa Highway Research Board Research Project HR-341, January 1993.
- [2] Strauss, P., Lourens, J. and van der Walt, J. : Performance of Thin Concrete Overlays in South Africa, 8th International Symposium on Concrete Roads, Theme IV, pp.133-138, Lisbon, Portugal, September 1998.
- [3] Salcedo, M. A.: Ultra-Thin Whitetopping Applications in Mexico, 8th International Symposium on Concrete Roads, Theme IV, pp.173-182, Lisbon, Portugal, September 1998.
- [4] Hitoshi MARUYAMA: Maintenance and Rehabilitation of Heavy Traffic Road Pavement at National Highway Route 23 (Thin layer pavement using SFRC), HOSOU, pp.16-21, May 1997.
- [5] Etsuro NODA and Yong-Jian KONG: The Interface Adhesion Shearing Stress of the Thin Layer Bonding Type Concrete Overlay on Asphalt Pavement, Proceedings of the 52th annual conference of Japan Society of Civil Engineers, 5, pp.94-95, September 1997.
- [6] Tatsuo NISHIZAWA, Syuichi KOKUBUN and Tsutomu FUKUTE: Dynamic Model of Thin Layer Concrete Overlay, Proceedings of the 53th annual conference of Japan Society of Civil Engineers, 5, pp.98-99, October 1998.
- [7] Shigeru IWAMA: Experimental studies on Structural Design of Concrete Pavement (3), Report of the public works research institute, Ministry of Construction, December 1962.
- [8] Tadashi FUKUDA: Mechanics of Stress Distribution in Concrete Pavements, Proceedings of the Japan Society of Civil Engineers No.242, pp.63-72, October 1975.
- [9] The Civil Aviation Bureau, Ministry of Transport: Outline for Structural Designs of Airport Concrete Pavement, pp.107-108, 1990.
- [10] Robert G. Packard: Structural Design of Concrete Pavements with Lean Concrete Lower Course, Proceedings of 2nd International Conference on Concrete Pavement Design, pp.119-131, 1981.
- [11] JPO Information: No.54--157123, December 11, 1979.
- [12] Etsuro NODA, Yong-Jian KONG and Yoshinori KASAHARA: Ultra-Thin Whitetopping, Journal of Pavement Engineering, JSCE Vol.2, pp.45-52, December 1997.
- [13] Larsen, T. J.: A Composite Pavement Design Procedure, Proceedings of 2nd International Conference on

Concrete Pavement Design, pp.99-105, 1981.

[14] Ghosh, R. K. and Garg, A. K.: Shear Stress in Concrete Pavements – Analytical Procedure for Highways and Airfields, Civil Engineering and Works Review, pp.577-582, June 1969.

[15] Ghosh, R. K. and Phull, Y. R.: Bonded Concrete Overlays, Civil Engineering and Public Works Review, pp.821-826, Aug. 1972.

[16] Tatsuo NISHIZAWA, Syuichi KOKUBUN and Tsutomu FUKUTE: Analysis Method for Composite Pavement Based on Elastic Plate FEM, Proceedings of the Japan Society of Civil Engineers No.613/V-42, pp.237-247, February 1980.

[17] Ronald Hudson, W. and Hudson Matlock: Analysis of Discontinuous Orthotropic Pavement Slabs Subjected to Combined Loads, HRR131, pp.1-48, 1966.

[18] Japan Society of Civil Engineers: The Structural Mechanics Handbook, pp.173-179, 1994.

[19] Riichirou ARAI: Applied Mechanics, pp.60-62, 1972. Gihoudo

[20] Japan Society of Civil Engineers: Pavement Engineering, pp.107-108, 1995.

[21] CHUUBU Road Research Group, Report of CHUUBU Road Research Group, pp.19-31, June 18, 1983.

[22] Hiromitsu NAKANISHI, Shinichi TAKEI and Hidekazu MAEDA: A Study on the Structural Evaluation for SFRC Thin Layer Pavement by Composite Beam Theory, Proceedings of the 53th annual conference of Japan Society of Civil Engineers, 5, pp.52-53, September 1998.

[23] Kano UESHITA, Toru YOSHIKANE and Tomio TAMANO: Analysis of Pavement Structures Measured by Core Boring and the Benkelman Beam Test, Journal of Materials, Concrete Structures and Pavements, No.214, pp.17-25, June 1973.

[24] Katsuhisa SATO and Tsutomu FUKUDE: Structural Evaluation and Overlay Thickness Design of Airport Asphalt Pavements by Dynaflect, Proceeding of the Japan Society of Civil Engineers No.303, pp.109-118, November 1980.